ORIGINAL PAPER - CROSS-DISCIPLINARY PHYSICS AND RELATED AREAS OF SCIENCE AND TECHNOLOGY

Design and simulation of a mirror-mitigated thermal load on Korea-4GSR hard X-ray undulator beamline optics

Yongsam Kim[1] · Byeong Gwan Cho[1,2] · Tae Yeong Koo[1]

Abstract

The "4th generation storage ring" (4GSR) in Korea is expected to be 10–100 times brighter than Pohang Light Source II, and it gives hard X-ray undulator beamline a great advantage. In PLS-II hard X-ray undulator beamline, the first crystal of a double crystal monochromator is the first optics to handle the radiated X-ray power. However, the power and power density due to the smaller X-ray beam sizes and divergences from the Korea-4GSR are too high to handle for the first crystal itself. We present how to design a hard X-ray undulator beamline to reduce the thermal load on the first crystal of the monochromator and simulation results of a mirror-mitigated thermal loads on the Korea-4GSR hard X-ray undulator beamline optics.

Keywords Diffraction limited storage ring · 4th Generation storage ring · X-ray optics

1 Introduction

Since the successful operation of diffraction-limited-storage-ring MAX-IV, newly constructing or upgrading the synchrotrons had gained momentum. To keep up with this global trend, the diffraction limited storage ring was decided to be constructed in Chengju, Korea, and its construction starts from 2022. The diffraction limited storage ring, also known as 4th generation storage ring (4GSR), offers electron emittance smaller than photon's intrinsic emittance $\lambda/4\pi$ (λ, photon wavelength) in the hard X-ray regime. The 4GSR in Korea (Korea-4GSR) has almost 2 orders of magnitude increase in coherent fraction and brightness, and smaller source sizes compared to Pohang Light Source II (PLS-II) [1, 2]. The total flux of the Korea-4GSR is roughly twice higher, but its smaller X-ray source size results in two orders of magnitude of higher flux density. This tremendous improvement greatly impacts on the beamline design.

In early construction phase of Korea-4GSR, 10 beamlines are planed: 8 hard X-ray beamlines and 2 soft X-ray beamlines [1]. 7 of 8 hard X-ray beamlines are undulator beamlines. For a hard X-ray undulator beamline using a crystal monochromator, it is important to manage the thermal load on its first crystal specially in Korea-4GSR.

2 Beamline layout design

First of all, we present how to design a hard X-ray undulator beamline to mitigate the thermal load on the first crystal of the monochromator. Figure 1 is an intuitive representation of how to manage the thermal load on the first crystal with optical elements. We calculated the X-ray energy-dependent transmissivity and reflectivity of optical elements: 0.1 mm-thick diamond filter, Si(111) single crystal, Pt-coated mirror (Fig. 1a–c). The transmissivity and reflectivity are converted to the absorptivities (Fig. 1d–f). The shaded area is total absorptivity for each elements in the given X-ray energy range, which means that larger shaded area corresponds to higher thermal load on the element. The area of Fig. 1(e) is nearly shaded; only 9.5 keV of 1.3 eV width area is reflected. What it means is that the crystal needs to bear almost all thermal load.

In a conventional hard X-ray undulator beamline in PLS-II, the first Si crystal with a filter can handle the PLS-II undulator's thermal load, which is represented as in Fig. 1g. However, those in Korea-4GSR are so higher than the

✉ Yongsam Kim
  yongsam_kim@postech.ac.kr

1   Pohang Accelerator Laboratory, Pohang 37673, South Korea

2   Korea Research Institute of Standards and Science, Daejeon, 34113, South Korea
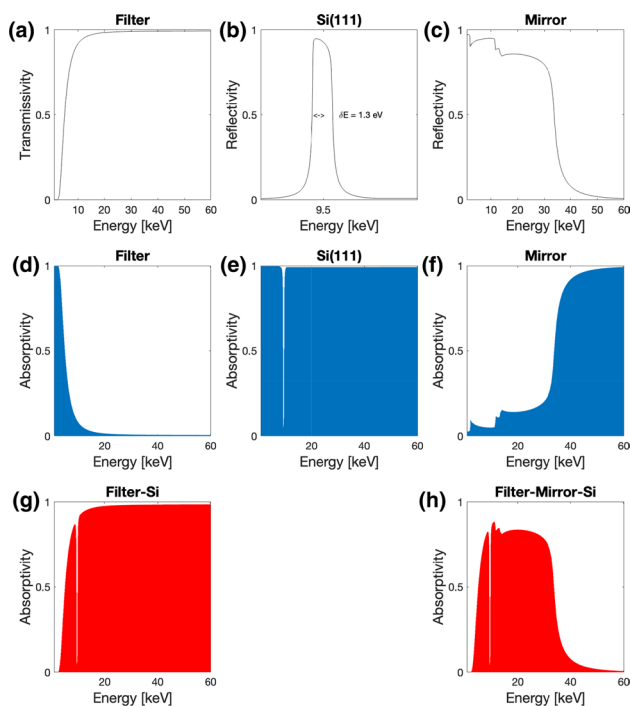
Fig. 1 Calculated transmissivity of **a** 0.1 mm diamond filter, and reflectivities of **b** Si(111) crystal at 9.5 keV and **c** Pt-coated mirror with 2.5 mrad incident angle. Schematic representations of the heat absorptivity of each optical elements (**d** 0.1 mm diamond filter, **e** Si(111) crystal, **f** Pt-coated mirror, and the combined heat absorption of the Si(111) crystal after **g** the filter only and **h** the filter and the mirror.

designed values that the first crystal cannot handle the thermal load. Therefore, an additional component is required to reduce the thermal load, which is a mirror [3]. The mirror is low band-pass filter (Fig. 1c). Most of the higher energy photons are absorbed (Fig. 1f). The coating materials and X-ray's incident angle of the mirror change the shaded area in the energy axis. Finally, the filter and mirror specification such as material, thickness, length, and position will determine the final absorptivity over the X-ray energy as in Fig. 1h, which will reduce the thermal load tremendously prior to the first crystal.

3 Thermal load simulation on Hard X-ray undulator beamline optics

For the detailed simulation, we suggest a Korea-4GSR hard X-ray undulator beamline layout in Fig. 2 based on the above concept. According to the Korea-4GSR conceptual design report [1], the X-ray energy range of most of hard X-ray undulator beamlines is within 5–40 keV and the beamline length is expected to be about 60–80 m (the length of the front end is about 25 m and its experimental hall is about

55 m). We put 2 m-long undulator with deflection parameter $K = 2$. The aperture is at 20 m from the source in the front end to use only central cone of the undulator radiation. Its opening size is 0.5×0.5 mm^2 which is full width of the photon beam size at 20 m. Since the designed X-ray energy range is above 5 keV, we put 0.1 mm-thick diamond window at 25 m to block the low-energy part in the radiation. The first Si mirror, Pt-coated vertical plane mirror with the incident angle of 2.5 mrad is placed at 30 m, and the second Si mirror, Pt-coated collimating vertical mirror at 35 m. Then, Si(111) double crystal monochromator (DCM) is placed at 40 m. The Pt-coating on the mirror and its 2.5 mrad incidence angle enable to pass the required X-ray energy (5–40 keV) downstream, since its reflectivity is about 80% at 32 keV (Fig. 1c). As shown in Fig. 1b, Si(111) bandpass is extremely narrow, so that the power and power density
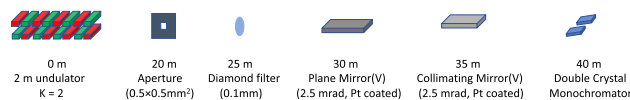

Fig. 2 A hard X-ray undulator beamline layout in Korea-4GSR
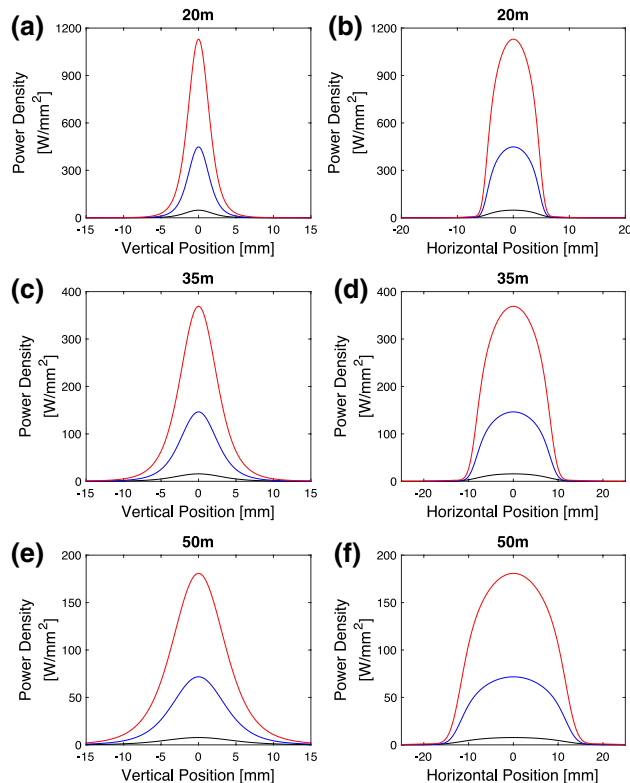

Fig. 3 Power density line profiles at 20 m (**a** vertical, **b** horizontal), 35 m (**c** vertical, **d** horizontal), 50 m (**e** vertical, **f** horizontal) from the source. g [red : Korea-4GSR 5 m-long undulator ($K = 2$), blue : Korea-4GSR 2 m-long undulator ($K = 2$), black : PLS-II 1.4 m long undulator ($K = 1.58$)]

after the first crystal can be ignored as the thermal load. Hence, we do not consider other optics in the layout down from the DCM. It is noteworthy to mention several points. (1) When a beamline uses no monochromator, pink beam, thermal load on all optics should be considered. (2) The number of mirrors prior to the monochromator and its facing direction could be changed due to the designed beamline specification, but we put two mirrors to deliver the X-ray beam parallel to the ground and adjust the beam divergence to the Si(111) crystal. (3) In the layout, we do not put any optics after the DCM, but one can put the designed focusing optics such as mirrors, compound refractive lens, zone plate, and so on. It is sure that this beamline layout safely covers the thermal load issue on the optics in most Korea-4GSR undulator beamlines, and it could be the standard layout for Korea-4GSR.

Now, we calculated the full power and power density using SPECTRA software [4]. The main storage ring parameters of the Korea-4GSR are in the reference [1]. The following Korea-4GSR hard X-ray undulator parameters are used for the simulation: 16 mm period, 2 m (or 5 m) length, and $K = 2$. Also, the storage ring parameters of PLS-II are in reference [5] and PLS-II 1C beamline undulator parameters are used: 20 mm period, 1.4 m length, and $K = 1.58$.

The calculated total powers from 5 m and 2 m-long undulators in the Korea-4GSR and 1.4 m-long undulator in the PLS-II are 36.0 kW, 14.3 kW, and 2.2 kW, respectively. To understand the detail of power distribution, the power density profiles from the several observation points are plotted in Fig. 3. At 20 m Fig. 3a, b, the power density maximums of the Korea-4GSR 5 m and 2 m-long undulator are 1.13 kW/mm^2 and 448 W/mm^2 which are 23.5 and 9.3 times higher than PLS-II 1C undulator's 48.1 W/mm^2. The higher increase in the power density than the total power is due to the smaller emittance, i.e., smaller source sizes and divergences of the Korea-4GSR [2]. The maximum power densities of 5 m- and 2 m-long Korea-4GSR undulator and PLS-II undulator at 35 m are 370 W/
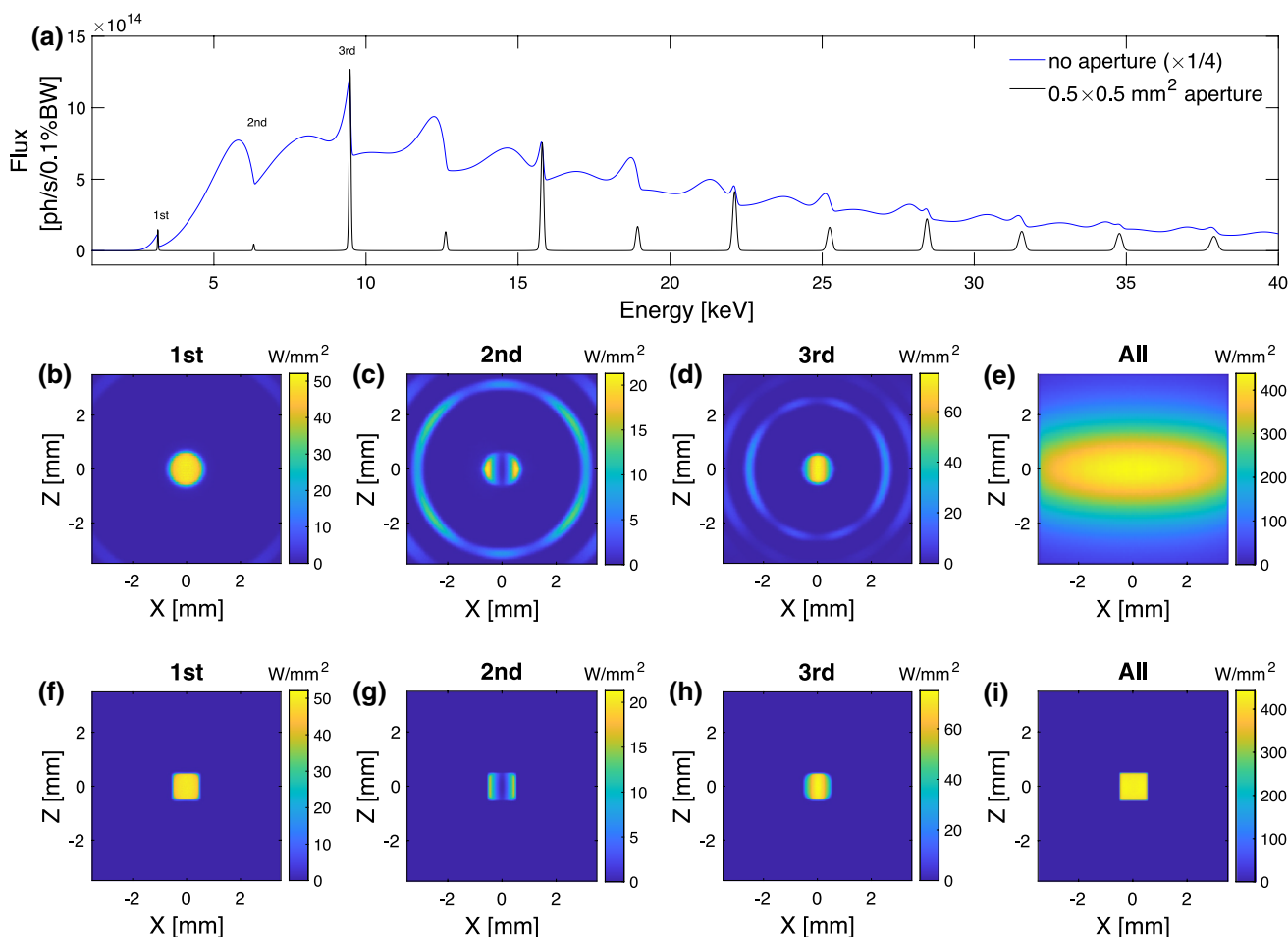

Fig. 4 **a** Calculated undulator spectra with (black) and without (blue) 0.5×0.5 mm^2 aperture at 20 m. Accumulated power density distribution at 20 m from the source of 1st harmonic (3.1–3.2 keV), 2nd harmonic (6.2–6.4 keV), 3rd harmonic (9.35–9.6 keV), and total (up to 60 keV) undulator radiation **b–e** without and **f–i** with the aperture, respectively

mm^2, 146 W/mm^2, and 16 W/mm^2 and those at 50 m are 180 W/mm^2, 72 W/mm^2, and 8 W/mm^2, respectively. The farther from the source point is, the lower the power density becomes. However, even at 50 m, the maximum power densities of 5 m- and 2 m-long Korea-4GSR undulators are much higher than that of PLS-II, so that it is required additional optics to reduce the power density [3].

The total power in Fig. 3 is calculated from the full radiation of the undulator without any filter or aperture. However, generally, the central cone of the undulator harmonic radiation is only used. Other parts are blocked by an aperture also known as white beam slits, fixed masks, or movable masks in the front end.

To calculate the detailed thermal load, power, and power density, on the optics from the apertured beam, we followed the recently developed simulation procedure for energy-dependent power density on OASYS (Orange Synchrotron Suite) environment [6, 7]. It calculates the spectral flux integrated over an aperture with 0.1% energy bandwidth and approximates the spectral flux in the energy interval δE, and calculates the power, $P_{\delta E}$ in the interval. Then, at every energy point, E_i, the shadow ray tracing algorithm in OASYS makes the histograms of the rays, Histogram(x,z) with each optical elements in the layout. The power of a single ray, $P_{ray,\delta E_i}$ (E_i) contains the interaction information from all optical elements, such as the incident, absorbed, and transmitted power density distribution on the elements [6]. As a result, the calculated power density (PD) is $PD_{\delta E_i}$ = Histogram(x,z) [$P_{ray,\delta E_i}$ (E_i) / $\delta x \delta z$].

Figure 4a shows the photon flux spectra with and without an aperture calculated by SRW (synchrotron radiation workshop) in OASYS. The simulated power density up to 60 keV with the calculating energy step 10 eV was 14.2 kW which is similar to the SPECTRA result, 14.3 kW. Even if we calculate the power density up to 90 keV, it increases by about 2%. Given the fact, we only simulated up to 60 keV of X-ray energy. Also, 0.1 mm-thick diamond filter at 25 m simply reduces the total power down to 13 kW. Then, 0.5× 0.5 mm^2 aperture further decreases the total power down to 420 W. The effect of the aperture on the total power reduction is demonstrated by the power density distributions of 1st (3.1–3.2 keV), 2nd (6.2–6.4 keV), and 3rd harmonic undulator radiations (9.35–9.6 keV) with and without the aperture (Fig. 4b–i). The calculation energy step for each undulator harmonic radiations with the filter was 1 eV. The total powers of 1st, 2nd, and 3rd harmonics are 85 W, 93 W, and 171 W without the aperture, and with the aperture, they goes down to 46 W, 7 W, and 52 W, respectively. Blocking non-central radiations by the aperture eliminates almost 97% of the total full power. However, as shown in Fig. 4e, i, the maximum power density (~440 W/mm^2) does not change, since it is in the central cone. Note that the maximum power density at 20 m with 0.1 mm diamond filter calculated by

SPECTRA is ~390 W/mm^2. This discrepancy could come from the approximation in calculating the power density with the energy step 10 eV and spatial distribution, but about 10% difference can be negligible in the thermal load context.

Then, this X-ray beam of the high power density is incident onto the first plane mirror with 2.5 mrad at 30 m (we assumed that the mirrors have no roughness and slope errors). The very low incident angle between the X-ray beam and the mirror surface makes its footprint spread in the beam propagation direction (Y) (Fig. 5a, b: its footprint on the mirror is due to the aperture). The spread footprint results in lowering the maximum power density to 0.4 W/mm^2 [8, 9]. About 30% of the incident power, 122 W is absorbed by the mirror, and the rest, 296 W is transmitted to the second collimating mirror at 35 m. Only 39 W is absorbed by the second mirror and most of the transmitted from the first mirror is transferred as it is. The absorbed maximum power density by the second mirror is smaller than 66 mW/mm^2. All the thermal loads on the mirrors are manageable by the conventional mirror cooling system [10, 11].

The energy setting of DCM was fixed at 9.5 keV which is in 3rd harmonic undulator radiation (Fig. 4a). The transmitted, 257 W, X-ray beam hits the first Si(111) single crystal with the incident angle 12.0°. Unlike the mirror, the Si(111) single crystal in DCM allows X-ray beam of the energy only satisfying Bragg's law to go downstream. Hence, almost all the power is absorbed by the first crystal (Fig. 5e): its
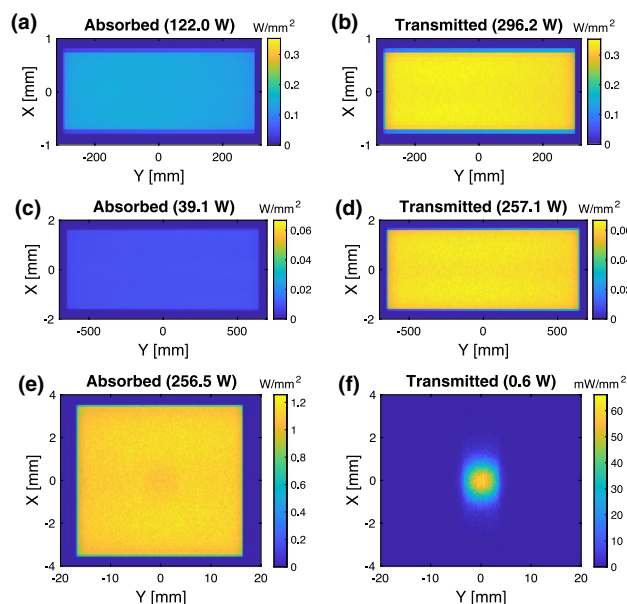

Fig. 5 Accumulated power density distribution on the first mirror (**a** absorbed, **b** transmitted), the second mirror (**c** absorbed, **d** transmitted) and the first Si(111) crystal of double crystal monochromator set at 9.5 keV (**e** absorbed, **f** transmitted)

Table 1 Summary of the total power and maximum power density from the layout

	*Unfiltered ×10³	Filtered ×10³	Apertured ×10³	1st Mirror Abs. (Trans.)	2nd Mirror Abs. (Trans.)	1st Si Abs. (Trans.)
Total Power [W]	14.2	13	0.42	122 (296.2)	39.1 (257.1)	256.5 (0.6)
Max. PD [mW/mm²]	448	440	440	148 (353)	10 (67)	1256 (66)

PD: power density, * : spectra calculation result of full radiation at 20 m, Abs: Absorbed, Trans: Transmitted

absorbed power and maximum power density are 256 W and 1.3 W/mm². Here, it is noteworthy that when the energy set in DCM changes to 2 keV, the incident angle turns to about 81.3°. It will increase the maximum power density by about 4.8 times, which is 6.2 W/mm². Even so, they are below those of 1.4 m-long undulator PLS-II 1C beamline [2]. The transmitted power from the 1st Si(111) crystal is 0.6 W and its maximum power density is 66 mW/mm². Consequently, we can safely ignore the thermal load of the downstream optics after the first Si(111) crystal.

4 Conclusions

We suggested a Korea-4GSR beamline layout that effectively mitigated the high power and power density, and simulated the thermal load on the X-ray optics. The 2 m-long undulator with the period 16 mm and deflection parameter ($K = 2$) shows the total power about 420 W and maximum power density ~440 W/mm² which are reduced by the 0.5× 0.5 mm² aperture and 0.1 mm-thick diamond filter. The first plane mirror spreads out the thermal load onto its surface with 2.5 mrad incidence angle and cuts down the maximum power density less than 0.4 W/mm². The transmitted power and power density from the second collimating mirror onto the first Si(111) crystal of the DCM is 257 W and less than 1.3 W/mm² on the first crystal (all values are summarized in Table 1). Both absorbed thermal load on the mirrors and the first crystal is manageable. Even if the length of the undulator increases to 5 m and the diamond filter becomes thinner, the current cooling system could handle the thermal loads in the layout.

References

1. K.W. Kim *et al.*, *PAL-PUB-2020-004* (Pohang Accelerator Laboratory, 2020)
2. B.-G. Cho, Y. Kim, S. Shin, T.-Y. Koo, J. Korean Phys. Soc. **78**, 467 (2021)
3. H. Wang, AIP Adv. **9**, 085007 (2019)
4. T. Tanaka, H. Kitamura, J. Synchrotron Rad. **8**, 1221 (2001)
5. PAL, *PLS-II PARAMETER HANDBOOK* (Pohang Accelerator Laboratory, 2011)
6. L. Rebuffi, X. Shi, M. Sanchez del Rio, R. Reininger, J. Synchrotron Rad. **27**, 1108 (2020)
7. M. Snchez del Rio, L. Rebuffi, AIP. Conf. Proc. **2054**, 060081 (2019)
8. A. Aquila, R. Sobierajski, C. Ozkan, V. Hájková, T. Burian, J. Chalupský, L. Juha, M. Störmer, S. Bajt, M.T. Klepka, P. Dłużewski, K. Morawiec, H. Ohashi, T. Koyama, K. Tono, Y. Inubushi, M. Yabashi, H. Sinn, T. Tschentscher, A.P. Mancuso, J. Gaudin, Appl. Phys. Lett. **106**, 241905 (2015)
9. T. Koyama, H. Yumoto, H. Miura, K. Tono, T. Togashi, Y. Inubushi, T. Katayama, J. Kim, S. Matsuyama, M. Yabashi, K. Yamauchi, H. Ohashi, Review of Scientific Instruments 87:5, 051801 (2016)
10. L. Zhang, R. Barrett, K. Friedrich, P. Glatzel, T. Mairs, P. Marion, G. Monaco, C. Morawe, T. Weng, Journal of Physcis: Conference Series **425**, 052029 (2013)
11. J.J. Knopp, M.V. Fisher, Z. Liu, J. Maser, R. Reininger, X. Shi, Mechanical Engineering Design of Synchrotron Radiation Equipment and Instrumentation **10**, 238 (2018)